npg

ORIGINAL ARTICLE

Preparation of a nanocomposite of magnetic, conducting nanoporous polyaniline and hollow manganese ferrite

Seyed Hossein Hosseini[1], Rahmatollah Rahimi[2] and Hamed Kerdari[3]

A nanocomposite of conducting, protonated, polyaniline and hollow $MnFe_2O_4$ was successfully synthesized by *in situ* self-assembly polymerization. First, core-shell hollow spheres of $MnFe_2O_4$ were fabricated by template polymerization, in which ferrite nanoparticles were coated onto the surface of functionalized core polystyrene (PS) spheres, and the core polymer was subsequently removed by calcination. Fourier transform infrared spectroscopy spectra of the ferrite-coated PS spheres and $MnFe_2O_4$ hollow spheres confirmed the elimination of the organic template after calcination. Scanning electron microscopy images revealed that the resultant composite was structurally nanoporous. The shape and holes of the $MnFe_2O_4$ spheres were investigated by transmission electron microscopy. In addition, the magnetic properties of the nanocomposite and $MnFe_2O_4$ were characterized on a vibrating sample magnetometer with maximum saturation magnetization values of 1.59 and 66.7 emu g^{-1}, respectively. The X-ray diffraction patterns of the ferrite sample agreed well with the standard pattern of the cubic structure. Atomic force microscopy was used for surface morphology analysis.

INTRODUCTION

As a classic conducting polymer, polyaniline (PANi) has recently been the center of great attention. It is known that PANi has a variety of oxidation states, three of which are commonly referred to in the literature: leucoemeraldine base (fully reduced), emeraldine base (half-oxidized) and pernigraniline base (fully oxidized). Emeraldine base is the most attractive because it can be doped with protonic acid to become emeraldine salt, and the DC conductivity of emeraldine salt is higher owing to charge delocalization across the polymer chain produced by doping H$^+$.[1,2] Nanostructured-conducting polymer composites have attracted significant scientific and technological interest because of their potential applications in various domains, for example, as microwave-absorbing materials and electromagnetic interference shielding.[3,4] Among conductive polymer composites, materials decorated with inorganic nanoparticles such as Al_2O_3,[5] γ-Fe_2O_3,[6] RuO_2[7] and TiO_2[8] have received a great deal of attention owing to possible interactions between inorganic nanoparticles and the polymeric matrix that may produce novel physical properties. Currently, there are many reports on the synthesis of composites containing PANi and magnetic oxides with various nanostructures, such as nanotubes, nanorods or core-shell nanostructures;[9–11] to the best of our knowledge, however, investigations on hollow or nanoporous composites have seldom been reported. Hollow magnetic nano-

spheres represent a class of materials that is of special interest in the fields of water purification, medicine and materials science.[12,13] In particular, the low densities of hollow spheres are expected to increase the stability of suspensions compared with those of solid particles. The strategies used to produce the magnetic hollow nanospheres are based mainly on two methods: (1) the sequential adsorption of magnetic nanoparticles onto colloidal hard templates, for example, silica[14] or polystyrene (PS) spherical nanoparticles,[15] and the further removal of the core either with the addition of a suitable solvent or by applying high temperature; and (2) emulsion synthesis using surfactants such as sodium dodecyl benzene sulfonate and cetyltrimethyl ammonium bromide.[16,17] In this paper, we report an extension of the sonochemical method used to prepare a PANi/hollow $MnFe_2O_4$ nanocomposite, and improve the stability and mixability of the suspension by dodecyl benzene sulfonic acid (DBSA) surfactant. All components using this method were uniformly dispersed under ultrasonication.

EXPERIMENTAL PROCEDURE

Materials and instruments

Monomers of aniline (Merck, Darmstadt, Germany) and styrene (Merck) were vacuum-distilled to remove inhibitor before use; acrylic acid (Aldrich, MO, USA, analytical purity) was used as received. Other chemicals, including metal salts, ethylene glycol, potassium persulfate, ammonium persulfate,

[1]Department of Chemistry, Islamic Azad University, Islamshahr Branch, Tehran, Iran; [2]Department of Chemistry, Iran University of Science and Technology, Tehran, Iran and [3]Department of Chemistry, Islamic Azad University, Saveh Branch, Saveh, Iran
Correspondence: Professor SH Hosseini, Department of Chemistry, Faculty of Science, Islamic Azad University, Islamshahr Branch, Namaz Square, Sayad shirazi Av., Tehran, Iran.
E-mail: shhosseini@iiau.ac.ir

hexamethylene tetraamine, potassium nitrate and DBSA were generally of reagent grade as obtained from commercial sources and were used without further purification. Water was deionized and deoxygenated before use.

The morphology of the particles was examined by scanning electron microscopy (Vega II model, Tescan, Cranberry Twp., PA, USA) and transmission electron microscopy (ZWISS EM900, Carl ZEISS AG, Oberkochen, Germany). Fourier transform infrared spectroscopy (FTIR) spectra were recorded on a Perkin–Elmer spectrum FTIR using KBr pellets (Perkin Elmer, MA, USA). Atomic force microscopy (AFM, Nano Scope II from Digital Instruments, Santa Barbara, CA, USA in contact mode) was used to analyze the surface morphology of the composite. Hollow particles of ferrite were examined by X-ray diffraction (Jeol JDX-8030, Jeol, Tokyo, Japan, operated at 30 kV and 20 mA). A vibrating sample magnetometer (Lakeshore, Westerville, OH, USA) was used to study the magnetic properties of the ferrite particles and the composite. Conductivity changes were measured with a four-probe device (ASTM Standards, F 43–93).

Synthesis of polystyrene–acrylic acid copolymer

Negatively charged PS spheres used as core particles were prepared by a free-emulsion polymerization method. A volume of 5 ml of styrene (0.044 mol) and 1 ml of acrylic acid (0.015 mol) were added to a flask with 50 ml deionized water. To eliminate oxygen effects, the solution was purified with nitrogen for 15 min under gentle stirring; the polymerization process was then initiated by adding 0.03 g potassium persulfate. The mixture was heated to 72 °C under a nitrogen atmosphere while stirring with a magnetic stirrer. After 24 h, the mixture was cooled to room temperature, and a colloidal solution of functionalized PS spheres was prepared.

Preparation of MnFe$_2$O$_4$ coated on PS spheres

As per the typical preparation process,[18] 4 ml PS colloid solution was diluted in 400 ml deoxygenated distilled water and then mixed in a flask with 100 ml of a metal salt solution that included 3.98 g FeCl$_2$.4H$_2$O (0.02 mol) and 1.62 g MnCl$_2$.2H$_2$O (0.01 mol); the mixture was then agitated for 5 min, after which the flask was placed in an ultrasonic system for 10 min. Thereafter, 10 ml ethylene glycol was poured into the reaction solution and dispersed for an excess 15 min by ultrasonication; the mixture was incorporated with 8 g hexamethylene tetraamine and 1 g potassium nitrate. The flask was immediately heated to 85 °C under gentle stirring. The color of the mixture gradually changed to black-brown. After 3 h, the system was cooled to room temperature and poured into excess distilled water; magnetic particles were then deposited using a magnetic field. The precipitate was washed with distilled water several times and then dried in an oven at 70 °C for 12 h. The dried residue was ground to improve the calcination process.
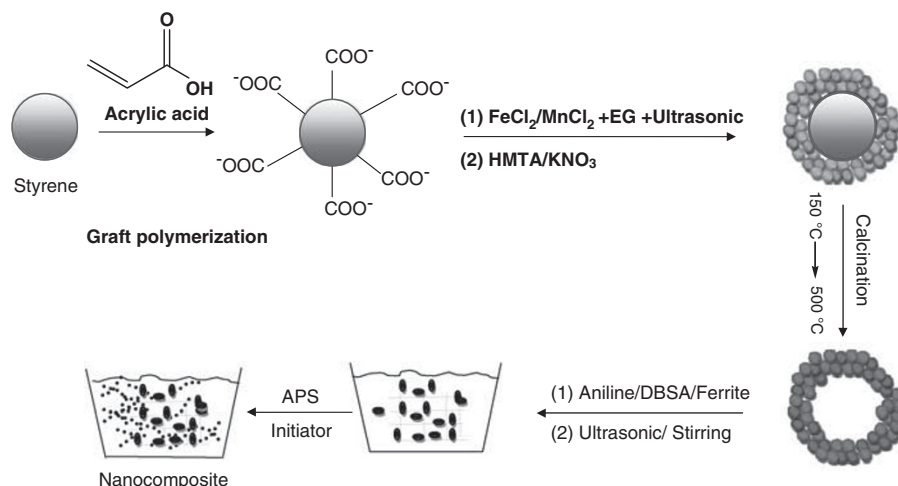
Preparation of hollow MnFe$_2$O$_4$ nanospheres

Hollow MnFe$_2$O$_4$ nanospheres were calcinated for 3 h under a nitrogen atmosphere at 500 °C.

The heating rate was 10 °C min^{-1}, below 150 °C, and 5 °C min^{-1}, between 150 and 500 °C.

Synthesis of nanoporous PANi and hollow MnFe$_2$O$_4$ nanocomposite

Four milliliters of aniline (0.044 mol) and 10 ml distilled water were mixed and agitated for 15 min. In another container, 5 g DBSA was diluted with 10 ml of deionized water to form a pulpy mixture. The solution was then poured into a solution of aqueous aniline; this emulsion was stirred for 1 h with a magnetic stirrer to form a homogenous phase.

In the next step, 5 ml of aqueous solution containing 0.6 g of hollow ferrite spheres was placed in an ultrasonic system for 10 min and added to the above suspension. The mixture was sonicated for an extra 15 min and then gently agitated using a mechanical stirrer for an additional 15 min; 10 ml of an aqueous solution containing 5 g of ammonium persulfate (0.022 mol) as oxidizing agent was slowly added (during 15 min) while stirring mechanically to initialize the polymerization reaction. The resulting green precipitate (PANi and hollow MnFe$_2$O$_4$ nanocomposite) was filtered, washed twice with distilled water and then dried overnight in an oven at 60 °C.

Preparation mechanism of nanoporous PANi and hollow MnFe$_2$O$_4$ nanocomposite

The formation mechanism of the nanoporous PANi/hollow manganese ferrite nanocomposite is schematically described in Scheme 1.

The first step in the synthesis of hollow MnFe$_2$O$_4$ nanospheres was the functionalization of the surfaces of PS by the graft polymerization of acrylic acid. We found that the carboxyl-functionalized groups could absorb Mn^{2+} and Fe^{2+} cations onto the surface of charged PS. The organic templates were then removed by sintering. In the next step, both non-homogeneous phases of inorganic nanoparticles and aniline monomers were mixed according to the proposed mechanism; DBSA is a surfactant having long hydrophobic and hydrophilic groups. This unique character is accompanied by the acidic proton of the SO$_3$H group when doping PANi. Aniline monomers, the aromatic base, are blended and protonated with surfactant to form the anilinium cation, which, aside from the hydrophilic group (SO$_3^-$) of DBSA, has a key role in the absorption of the Mn^{2+} and Fe^{2+} cations of ferrite. Although the magnetic nanoparticles tend to vigorously agglomerate, the long hydrophobic tail of DBSA prevents their agglomeration. Ammonium persulfate was then added to the mixture as an oxidizing agent to begin polymerization, and hollow MnFe$_2$O$_4$ nanoparticles were uniformly formed in the polymer base.
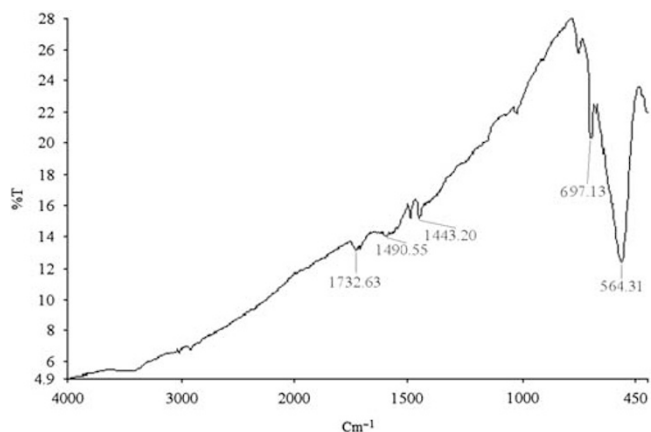

Scheme 1 Illustration of the possible formation mechanism of the nanoporous polyaniline and hollow manganese ferrite nanocomposite.

Figure 1 Fourier transform infrared spectroscopy spectrum of MnFe$_2$O$_4$ coated onto polystyrene (PS) spheres.
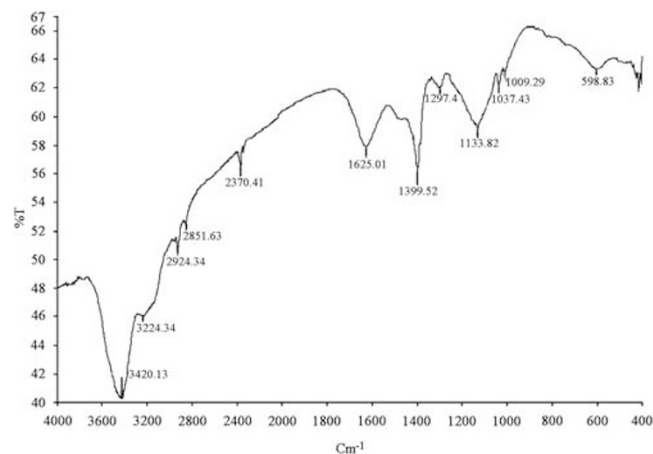

Figure 3 Fourier transform infrared spectroscopy spectra of the PANi and hollow MnFe$_2$O$_4$ nanocomposite.
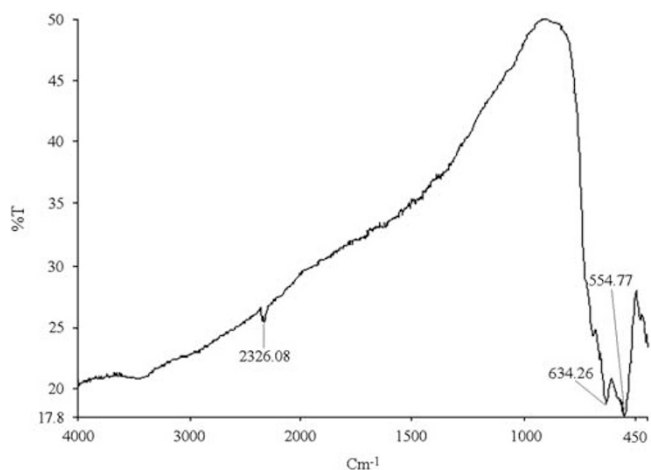

Figure 2 Fourier transform infrared spectroscopy spectrum of ferrite hollow spheres calcined at 500 °C.
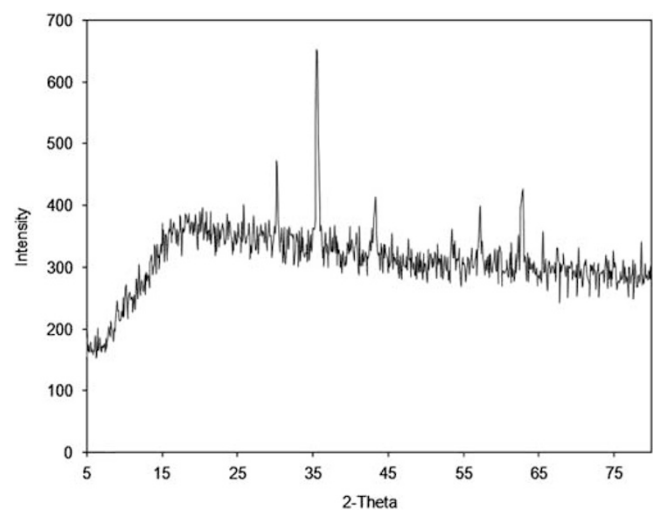

Figure 4 X-ray diffraction pattern of hollow MnFe$_2$O$_4$.

RESULTS AND DISCUSSION

Material characterization

Figure 1 shows the FTIR spectrum of MnFe$_2$O$_4$-coated functionalized PS spheres. The characteristic peak at 564.31 cm^{-1} corresponds to the Fe–O stretching vibration of ferrite. The typical absorption peaks at 697.13/~750 and 1443.20/1490.55 cm^{-1} are attributed to the out-of-plane bending vibration mode of the monosubstituted benzene ring group of PS and the benzene ring backbone mode in PS, respectively. The peak at 1732.63 cm^{-1} is a characteristic absorption of the vibration of the C=O bond in acrylic acid. A wide band in the spectrum of the coated PS spheres can be seen at ~3450 cm^{-1}, which is attributed to the hydroxyl groups in acrylic acid.

Figure 2 illustrates the FTIR spectrum of calcinated hollow MnFe$_2$O$_4$ nanoparticles. The peaks at 697.13/~750 cm^{-1}, 1443.20/1490.55 cm^{-1} and 1732.63 cm^{-1} are related to the charged PS, which disappear after calcination at 500 °C, indicating the formation of hollow spheres. The absorption peak of MnFe$_2$O$_4$ at 554.77 cm^{-1} becomes sharper after calcination.

Figure 3 shows the FTIR spectrum of the nanoporous PANi and hollow MnFe$_2$O$_4$ nanocomposite. The peaks at 1009.29 and 1037.43 cm^{-1} correspond to the S–O vibration of the DBSA residue as surfactant and dopant in the product. In addition, the S=O

symmetrical stretching vibration can be observed around 1133.82 cm^{-1}, which is broadened because of an overlap with vibrational modes of N=Q=N (Q refers to the quinonic-type rings) in the doped PANi chain. The typical peak of ferrite could overlap with the absorption peak of DBSA (598 cm^{-1}) at higher wave numbers than pure ferrite, indicating strong electrostatic interactions between MnFe$_2$O$_4$ nanoparticles and the SO$_3^-$ group. The observed peaks at 1625 and 1399.52 cm^{-1} are attributed to the C=C stretching deformation of quinoid and benzenoid rings, respectively. Under the typical state of PANi, these vibrations should be seen at 1490/1590 cm^{-1}; however, this shift can be related to the linking of oxygen atoms from the SO$_3^-$ functional groups to nitrogen atoms in the PANi chain.

Figure 4 demonstrates the X-ray diffraction pattern of the hollow ferrite spheres. The positions and relative intensities of all of diffraction peaks agree well with those of Fe$_3$O$_4$ and MnFe$_2$O$_4$, according to standard cards No. 19-0629, 10-0319 and 32-0637. The sharp peaks at 35.5, 30.2, 57.2 and 62.9° are attributed to magnetite, and the weak peaks at 18.1, 43.3 and 47.7° belong to manganese ferrite. The presence of magnetic indicators is because of the lower molar percentage of manganese chloride in the reaction compared with that of iron chloride. Therefore, the resulting compound is a mixture of MnFe$_2$O$_4$ and magnetite. The conditions used were

$\lambda = 1.54\,\text{Å}$ and $\beta = 0.30°$ or 0.005 radians. The average crystallite size of the MnFe$_2$O$_4$ particles was estimated, using the Scherer formula, to be 28.55 nm. On the basis of the results of the X-ray diffraction curve and the mentioned standard patterns, MnFe$_2$O$_4$ is expected to be a cubic system.

Morphology analysis

A scanning electron microscopy image of porous or hollow MnFe$_2$O$_4$ nanospheres and PANi-MnFe$_2$O$_4$ nanocomposite are displayed in Figures 5a and b. As shown in Figure 5a, there are numerous uniform spherical particles containing holes at the center of some spheres. In Figure 5b, it can be observed that the PANi and MnFe$_2$O$_4$ nanocomposite (15 wt%) still retains the morphology of PANi. It is unknown how a spongy composite can be formed through the polymerization process. The scanning electron microscopy image clearly shows that the MnFe$_2$O$_4$ was distributed rather homogeneously, and indicates that ultrasonication is effective in dispersing nanoparticles in the polymeric matrix. Figures 5c and d show transmission electron microscopy images of hollow MnFe$_2$O$_4$ nanospheres. According to the images, the shapes of the spheres are well retained during the heating process, and the holes at the centers of the spheres can be seen clearly. Therefore, hollow nanospheres were successfully generated by removing the organic template during the calcination process.

Figure 6 shows an AFM image of the surface structure of an as-prepared PANi-DBSA/hollow MnFe$_2$O$_4$ nanocomposite film containing 0.25 g of nanocomposite dissolved in 5 ml *N*-methyl-2-pyrrolidone solution. Numerous bumps can be observed on the surface of the composite, which indicates the presence of MnFe$_2$O$_4$ magnetic nanoparticles in the polymer. Agglomerations can be seen in some areas, which indicate the accumulation of magnetic particles resulting from the strong attraction between the nanoparticles.

Figure 7 shows a top-view AFM image of the nanocomposite, which is shown to contain numerous dots. These indicate the even
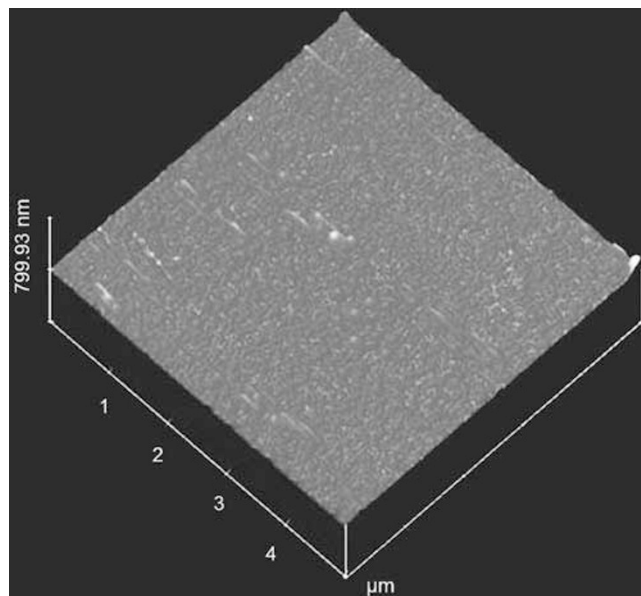

Figure 6 Atomic force microscopy image of the surface of the PANi and hollow ferrite nanocomposite. A full color version of this figure is available at *Polymer Journal* online.
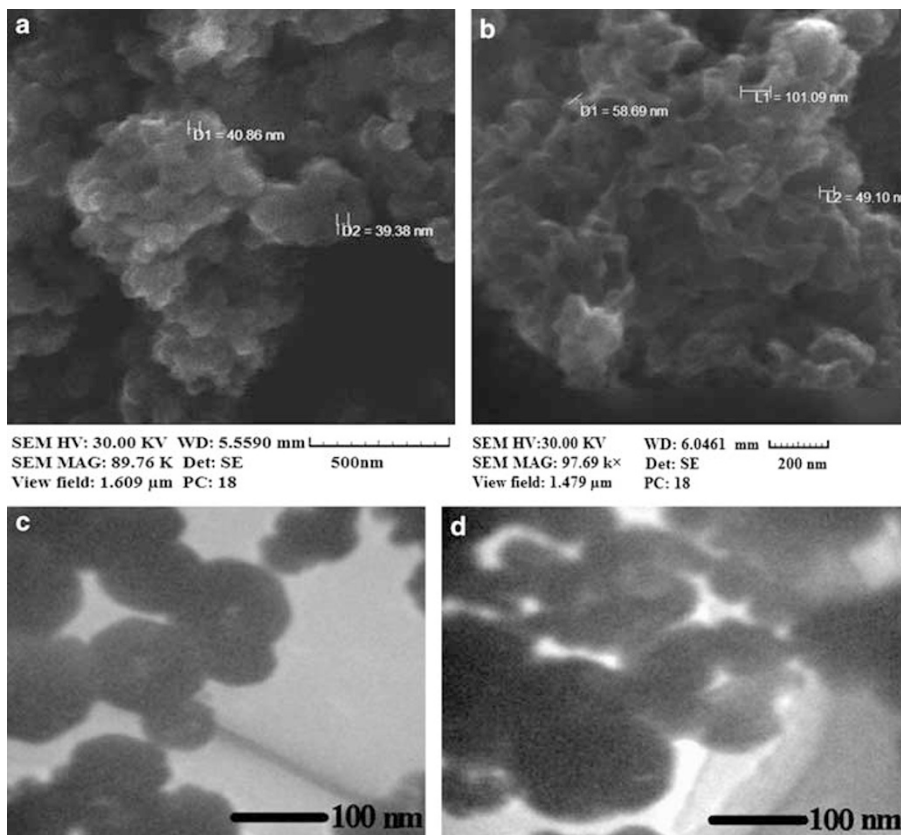

Figure 5 Scanning electron microscopy image of hollow MnFe$_2$O$_4$ nanospheres (**a**), nanoporous PANi and hollow MnFe$_2$O$_4$ nanocomposite (**b**), transmission electron microscopy images of hollow MnFe$_2$O$_4$ nanospheres (**c, d**).
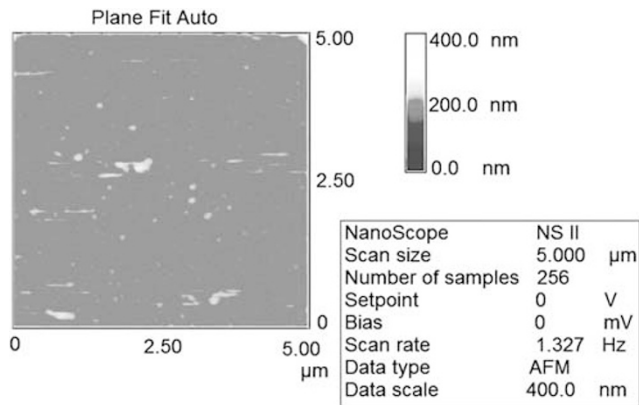
Figure 7 Atomic force microscopy image of the top surface of the PANi and hollow ferrite nanocomposite. A full color version of this figure is available at *Polymer Journal* online.
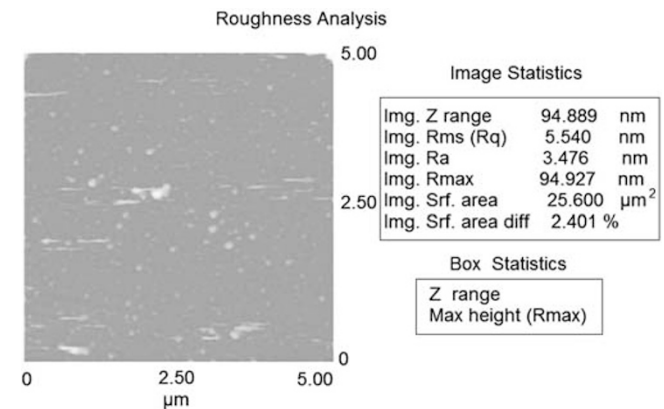

Figure 8 Atomic force microscopy image of the height of ferrite nanoparticles in the PANi and hollow ferrite nanocomposite. A full color version of this figure is available at *Polymer Journal* online.

Figure 9 Atomic force microscopy image of the width of ferrite nanoparticles in the PANi and hollow ferrite nanocomposite. A full color version of this figure is available at *Polymer Journal* online.

distribution of magnetic nanoparticles in the composite. The purple color indicates a size of 200 nm for the composite accumulation.

The AFM image in Figure 8 indicates the height of the MnFe$_2$O$_4$ particles. According to the image, the height of nanoparticles is estimated to be 23.66 nm. Figure 9 shows an AFM image that indicates

Figure 10 Atomic force microscopy image of the roughness of the PANi and hollow ferrite nanocomposite. A full color version of this figure is available at *Polymer Journal* online.
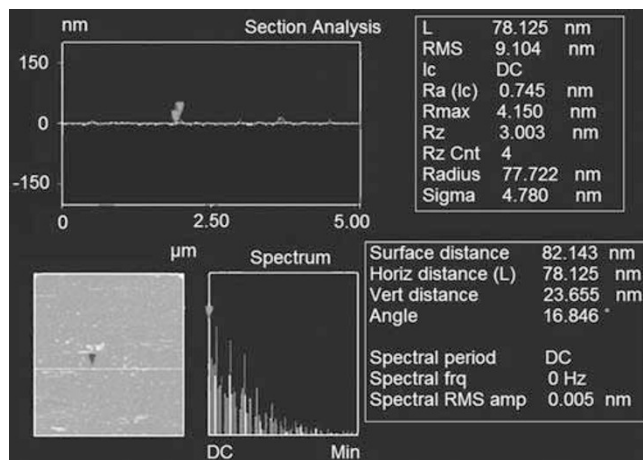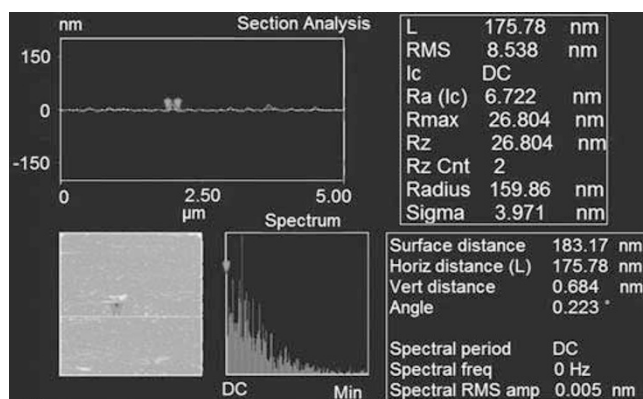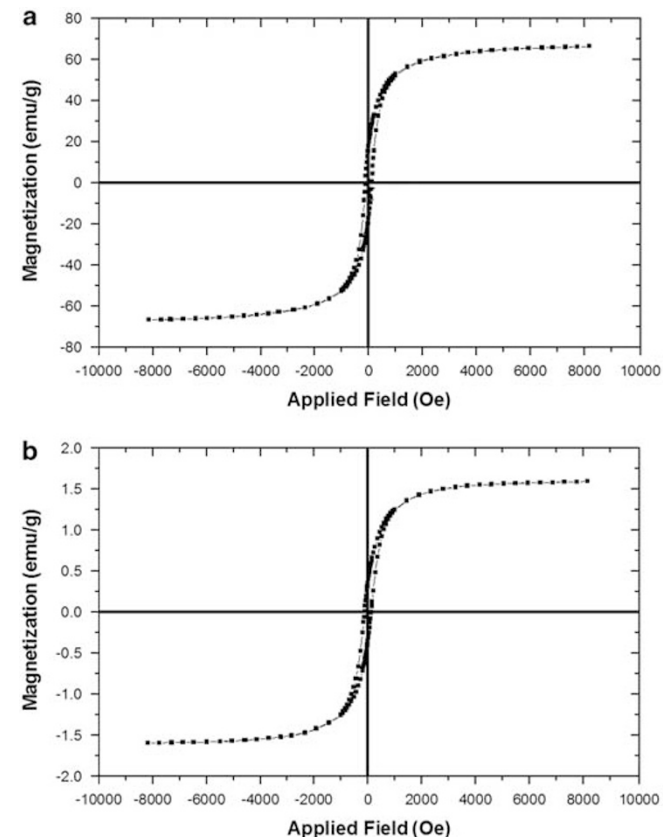

Figure 11 Magnetization curve of (**a**) hollow ferrite and (**b**) PANi and hollow MnFe$_2$O$_4$ nanocomposite.

the width of the MnFe$_2$O$_4$ particles. According to the image, the width of the nanoparticles is estimated to be 175.78 nm. Figure 10 shows an AFM image that indicates the roughness of the PANi and hollow MnFe$_2$O$_4$ nanocomposite. According to the image, the maximum amount of unevenness in the composite surface is estimated to be 94.927 nm.

Magnetic properties
Figures 11a and b show the magnetization (M) versus the applied magnetic field (H) for hollow MnFe$_2$O$_4$ and MnFe$_2$O$_4$/PANi nano-

composites (15 wt%), respectively. The magnetic properties of the hollow ferrite depicted in Figure 11a were analyzed by room-temperature vibrating sample magnetometer with an applied field of $-8.2 \leqslant H \leqslant 8.2$ kOe; the value of saturation magnetization (M_s) was ~ 66.7 emu g^{-1}, and the remnant magnetization (M_r) and coercivity field were 17.81 emu g^{-1} and 110 Oe, respectively.

Figure 11b shows clear saturation between $-8.2 \leqslant H \leqslant 8.2$ kOe, with a saturation magnetization (M_s) of ~ 1.59 emu g^{-1} and a remnant magnetization (M_r) of ~ 0.35 emu g^{-1} for the nanocomposite, which is lower than that of pure manganese ferrite nanoparticles. Thus, the magnetization curve of the sample shows weak ferromagnetic behavior, with slender hysteresis. The magnetic properties of nanocomposites containing magnetite or ferrite particles have been believed to be highly dependent on sample shape, crystallinity and the number of magnetic particles; therefore, they can be adjusted to obtain the optimum properties.

Conductivity properties

The conductivity of the PANi and hollow MnFe$_2$O$_4$ nanocomposite doped with DBSA surfactant was assessed using a four-probe conductivity-assessing device; the average conductivity, as determined by the assessments, was 1.10 S cm^{-1}. This reveals that the acidic hydrogen of the -SO$_3$H group in DBSA has a good ability to dope PANi.

CONCLUSION

In summary, a PANi and MnFe$_2$O$_4$ nanocomposite containing hollow ferromagnetic nanoparticles has been synthesized. This report provides a method to improve the mixability of inorganic particles with an organic phase. AFM images indicate the even distribution of MnFe$_2$O$_4$ in a PANi base, which proves the effectiveness of DBSA and ultrasonic devices in mixing two non-homogeneous phases. Generally, conducting PANi-containing magnetic materials are applied as an electromagnetic interference shielding. In this study, we composed a nanoporous PANi and hollow Mn-Fe$_2$O$_4$ nanocomposite that possesses enhanced microwave-absorbing properties owing to the nanoporous structure of PANi and the hollow ferrite spheres.

1   Stejskal, J. & Gilbert, R. G. Polyaniline preparation of a conducting polymer. *Pure Appl. Chem.* **74,** 857–867 (2002).
2   Hosseini, S. H., Abdi Oskooe, S. H. & Entezami, A. A. Toxic gas and vapour detection with polyaniline gas sensors. *Iranian Polym. J.* **14,** 333–344 (2005).
3   Yang, C., Li, H., Xiong, D. & Cao, Z. Hollow polyaniline/Fe$_3$O$_4$ microsphere composites: preparation, characterization, and applications in microwave absorption. *React. Funct. Polym.* **69,** 137–144 (2009).
4   Saini, P., Choudhary, V., Singh, B. P., Mathur, R. B. & Dhawan, S. K. Polyaniline–MWCNT nanocomposites for microwave absorption and EMI shielding. *Mater. Chem. Phys.* **113,** 919–926 (2009).
5   Teoh, G. L., Liew, K. Y. & Mahmood, A. K. Preparation of polyaniline-Al$_2$O$_3$ composites nanofibers with controllable conductivity. *Mater. Lett.* **61,** 4947–4949 (2007).
6   Singh, K., Ohlan, A., Kotnala, R. K., Bakhshi, A. K. & Dhawan, S. K. Dielectric and magnetic properties of conducting ferromagnetic composite of polyaniline with γ-Fe$_2$O$_3$ nanoparticles. *Mater. Chem. Phys.* **112,** 651–658 (2008).
7   Rao, R. K. & Vijayan, M. Ruthenium (II)-mediated synthesis of conducting polyaniline (PANi): a novel route for PANi–RuO$_2$ composite. *Synthetic Met.* **158,** 516–519 (2008).
8   Radhakrishnan, S., Sijua, C. R., Mahanta, D., Patil, S. & Madras, G. Conducting polyaniline–nano-TiO$_2$ composites for smart corrosion resistant coatings. *Electrochim. Acta.* **54,** 1249–1254 (2009).
9   Zhang, Z. & Wan, M. Nanostructures of polyaniline composites containing nano-magnet. *Synth. Met.* **132,** 205–212 (2003).
10 Yang, Q. L., Zhai, J., Feng, L., Song, Y. L., Wan, M. X., Jiang, L., Xu, W. G. & Li, Q. S. Synthesis and characterization of conducting polyaniline/γ-Fe$_2$O$_3$ magnetic nanocomposite. *Synth. Met.* **819,** 135–136 (2003).
11 Jacobo, S. E., Aphesteguy, J. C., Anton, R. L., Schegoleva, N. N. & Kurlyandskaya, G. V. Influence of the preparation procedure on the properties of polyaniline based magnetic composites. *Eur. Polym. J.* **43,** 1333–1346 (2007).
12 Iram, M., Guo, C., Guan, Y., Ishfaq, A. & Liu, H. Adsorption and magnetic removal of neutral red dye from aqueous solution using Fe$_3$O$_4$ hollow nanospheres. *J. Hazard Mater.* **181,** 1039–1050 (2010).
13 Figuerola, A., Corato, R. D., Manna, L. & Pellegrino, T. From iron oxide nanoparticles towards advanced iron-based inorganic materials designed for biomedical applications. *Pharmacol. Res.* **62,** 126–143 (2010).
14 Liu, J., Deng, Y., Liu, C., Sun, Z. & Zhao, D. A simple approach to the synthesis of hollow microspheres with magnetite/silica hybrid walls. *J. Colloid Interf. Sci.* **333,** 329–334 (2009).
15 Yang, H., Jiang, W. & Lu, Y. Fabrication and characteristic of conductive and ferromagnetic hollow composite microcapsules. *Mater. Lett.* **61,** 2789–2793 (2007).
16 Zhang, D., Tong, Z. W., Li, S. Z., Zhang, X. B. & Ying, A. Fabrication and characterization of hollow Fe$_3$O$_4$ nanospheres in a microemulsion. *Mater. Lett.* **62,** 4053–4055 (2008).
17 Ni, S., Lin, S., Pan, Q., Yang, F., Huang, K., Wang, X. & He, D. Synthesis of core–shell α-Fe$_2$O$_3$ hollow micro-spheres by a simple two-step process. *J. Alloy. Compd.* **478,** 876–879 (2009).
18 Zhang, Y., Huang, Z., Tang, F. & Ren, J. Ferrite hollow spheres with tunable magnetic properties. *Thin Solid Films* **515,** 2555–2561 (2006).